

Word count (2,011)

**TITLE:**

A 71-year-old man with dyspnea and cough during chemotherapy

**SHORT TITLE:**

An elderly man with dyspnea and cough

**AUTHORS:**

Kazuko Yamamoto, MD<sup>1</sup>; Koji Ando, MD<sup>2</sup>; Moe Tanaka, MD<sup>1</sup>; Hirokazu

Yura, MD<sup>1</sup>; Noriho Sakamoto, MD<sup>1</sup>; Yoshiaki Zaizen, MD<sup>3</sup>; Kazuto

Ashizawa, MD<sup>4</sup>; Junya Fukuoka, MD<sup>3</sup>; Yasushi Miyazaki, MD<sup>2</sup>; Hiroshi

Mukae, MD<sup>1</sup>

**AFFILIATIONS:**

1) Department of Respiratory Medicine, Nagasaki University Graduate School of Biomedical Sciences, Nagasaki, JAPAN, 2) Department of Hematology, 3) Department of Pathology, 4) Department of Clinical Oncology, Nagasaki University Hospital, Sakamoto 1-7-1, Nagasaki, JAPAN 852-8102

**CORRESPONDENCE:**

Kazuko Yamamoto MD, PhD

Department of Respiratory Medicine, Nagasaki University Graduate School of Biomedical Sciences,

Sakamoto 1-7-1, Nagasaki, JAPAN 852-8102

e-mail: [kazukomd@nagasaki-u.ac.jp](mailto:kazukomd@nagasaki-u.ac.jp)

**CONFLICT OF INTEREST:**

No authors have any conflict of interest to disclose.

**KEY WORDS:**

Metastatic pulmonary calcification, multiple myeloma, acute respiratory  
distress syndrome

## Case Presentation

A 71-year-old Japanese male ex-smoker, with a 3-year history of light chain ( $\lambda$ ) multiple myeloma, Durie-Salmon stage III, presented with increasing dyspnea and cough of two weeks' duration in the course of chemotherapy (lenalidomide and dexamethasone) for relapsed disease. He had recently undergone total thyroidectomy combined with parathyroidectomy for thyroid papillary carcinoma. He was admitted to the local hospital because he presented with fever, pyuria, dehydration, and marked hypercalcemia (corrected serum calcium of 15.9 mg/dL) during chemotherapy. Although his fever and pyuria cleared following ceftriaxone treatment for urinary tract infection, and hypercalcemia and dehydration also rapidly improved upon intravenous isotonic fluid and calcitonin administration, he had worsening cough and dyspnea, with bilateral lung opacities on a chest radiograph, and he was referred to our hospital for further examination and treatment.

Physical examination revealed an afebrile man in acute respiratory distress.

He was alert, with blood pressure 137/98 mmHg, pulse 53 beats/min,

temperature 97.5°F, respiratory rate 20 breaths/min, and oxygen saturation 95% breathing 4 L of nasal oxygen at rest. He had bilateral jugular vein distention, and bilateral coarse crackles during inspiration and a bilateral wheeze during expiration were heard on chest auscultation. Cardiovascular exam demonstrated a normal cardiac rhythm without murmurs, rubs, or gallops. No neurological deficits, peripheral edema, or skin lesions were observed.

His complete blood count revealed a white blood cell count of 7,400 cells/mm<sup>3</sup>, hemoglobin 11.8 g/dL, and platelet count 20.9 × 10<sup>4</sup>/mm<sup>3</sup>. Serum chemistry showed a blood urea nitrogen (BUN) level of 16.0 mg/dL, creatinine 1.69 mg/dL, total protein 5.2 g/L, albumin 2.2 g/L, immunoglobulin G 318 mg/dL (normal value range: 861-1,747 mg/dL), free light chain (FLC) κ 18.5 mg/dL (normal value range: 3.3-19.4 mg/dL), FLC λ 2,310 mg/dL (normal value range: 5.7-26.3 mg/dL), FLC κ/λ ratio 0.008 (normal value range: 0.26-1.65), corrected calcium 10.3 mg/dL, phosphorus 2.5 mg/dL, intact parathyroid hormone 9.8 pg/mL, alkaline phosphatase 860 U/L, and N-terminal

pro-brain natriuretic peptide 23,721 pg/mL. His blood gas test with nasal oxygen inhalation of 3L/min revealed pH 7.445, PaO<sub>2</sub> 78.3 Torr, PaCO<sub>2</sub> 37.1 Torr, HCO<sub>3</sub> 25.0 mmol/L, and AaDO<sub>2</sub> 103 Torr.

A chest radiograph showed dense areas of consolidation sparing right mid lung zone and bases, sternotomy clips, enlarged cardiac contour, subpleural opacities bilaterally, especially in the upper third of the lung zones, and small bilateral pleural effusions (Fig 1A). A trans-thoracic echocardiogram revealed an ejection fraction within normal range and a slightly dilated left ventricle in diastole (61 mm). A chest computed tomography (CT) scan showed bilateral high-attenuated consolidation with air bronchograms, mainly in peripheral distribution, with some extending centrally in a peribronchovascular distribution, with sparing of the subpleural regions in the periphery of the lower area of the lungs. Small nodular ground-glass opacities were seen in the lungs bilaterally, none of which had been detected on CT that was performed 2 weeks before admission. Multiple bilateral pleural calcifications and calcifications of the myocardium at the side of the

ventricular septum were observed, and bilateral pleural effusions were also noted (Fig. 2A, 2B). The patient underwent <sup>99m</sup>Techneium (Tc) diphosphonate bone scintigraphy, which revealed diffuse accumulation in the thorax, with significant abnormal increased activity in the lungs and myocardium (Fig. 3C).

In summary, this patient was an elderly man who underwent chemotherapy for multiple myeloma, showed progressive dyspnea and cough over two weeks; diffuse consolidation in bilateral lungs with <sup>99m</sup>Tc uptake by bone scan were detected. To determine a diagnosis, he underwent bronchoscopy. Multiple white elevated nodular lesions were seen in the trachea and in the endobronchial membranous portion (Fig 3A, 3B). Bronchoalveolar lavage (BAL) performed from the right middle lobe revealed an increased total cell count ( $3.65 \times 10^5/\text{mL}$ ), which was within the normal range for cellular differentiation. The BAL fluid was also negative for malignant cells, mycobacterium and pneumocystis, and bacterial and fungal cultures. Endobronchial mucosal biopsy from the right upper bronchus showed

basophilic fine calcific substances along the thickened parabronchial interstitial space (Fig. 4A). Transbronchial lung biopsies from the right lower lobe, showed multiple clusters of polypoid organization in airspaces, most of which were associated with basophilic string-shaped calcifications at the base of their stalk. Those calcifications were observed in the alveolar septa, and the alveolar walls were thickened (Fig. 4B). Von Kossa staining highlighted extensive deposition of amorphous calcium salts alongside areas of organizing pneumonia (OP) (Fig. 5A). Further Elastica van Gieson (EVG) staining revealed temporally heterogeneous, acute and subacute, collagenous depositions in areas of OP (Fig. 5C) and chronic fibrotic scars attached to the calcifications (Fig. 5D).

*Q: What is the diagnosis?*

*A: Diagnosis: Metastatic pulmonary calcification*

Discussion

## Clinical Discussion

Metastatic pulmonary calcification (MPC) is characterized by the deposition of calcium salts in the lungs under metabolic conditions producing an elevated calcium-phosphate product. MPC is one of multiple conditions that may present as calcifications in the lungs, and are differentiated from dystrophic calcifications made by injured or necrotic tissues at normal serum calcium levels in infectious diseases (tuberculosis, pneumocystis), noninfectious granulomatous diseases (e.g., sarcoidosis), or vascular coagulation (Table 1)<sup>1</sup>. The clinical manifestations of MPC are usually minimal, but fatal acute lung injury (ALI) with MPC in myeloma patients has been reported<sup>2,3,4</sup>. Increased renal tubular calcium reabsorption and decreased glomerular filtration rate, resulting in elevated calcium-phosphate product<sup>5</sup>, and excessive osteolysis in myeloma patients may also relate to the pathogenesis of aggressive MPC. In our patient, the rapid decline in serum calcium levels during calcitonin infusion and progressive renal failure due to infection and dehydration before admission

to our hospital were most likely the causes of rapid MPC development, in addition to the hyperphosphatemia caused by hypoparathyroidism following parathyroidectomy<sup>6</sup>. Pathological findings suggest that ALI developed due to organizing pneumonia surrounded by the disseminated calcifications. Cough, dyspnea, and hemoptysis are nonspecific common clinical symptoms of MPC, but in our patient, echocardiography and bronchoscopy excluded most of the differential diagnoses that were considered, such as heart failure, pulmonary edema, drug-induced pneumonia, and atypical pneumonia. Calcium precipitation in the lungs due to ceftriaxone infusion<sup>7</sup> was not likely in our case either because the calcification pattern differed (not embolic) and respiratory symptoms worsened despite the decline of serum calcium levels. The reversal of calcifications did not occur either during or after alfacalcidol treatment. The mechanism of hypoxemia in our patient may have been induced by diffuse OP packed in the alveolar spaces, which were the result of desmoplastic changes made by multiple calcifications in the alveolar septa. Although only a few reports have addressed bronchoscopic findings of MPC<sup>8,9</sup>,

bronchoscopy was useful for diagnosis in our case. Endobronchial mucosal nodules raise the differential diagnosis of tracheopathia osteopathica, amyloidosis, sarcoidosis, Crohn's disease, Wegener granulomatosis, and infection (papillomatosis, rhinoscleroma, tuberculosis, and fungi) <sup>10</sup>.

The patient was treated for over 10 days with 1 µg of alfacalcidol, ferric citrate hydrate, and precipitated calcium, which improved his hypoxemia and respiratory symptoms, and was discharged on day 29. A chest CT scan performed 3 months later revealed that the consolidations and calcifications had disappeared in the lungs (Fig. 2C). Successful treatment of MPC in a patient with myeloma involves decreasing serum calcium levels with bisphosphonate or chemotherapy to treat the myeloma itself.

### Radiologic Discussion

A chest radiograph, which is not specific for the diagnosis of MPC, may show confluent or patchy airspace opacities suggesting pulmonary edema or pneumonia, as seen in our patient<sup>11</sup>. Chest CT, particularly high-resolution

CT (HRCT), has excellent sensitivity for MPC detection. The HRCT pattern may indicate MPC in the upper lobes of the lung, associated with an increase in alkalinity resulting from higher blood pH and lower PaCO<sub>2</sub> at the apex compared to that at the base due to the increased ventilation-perfusion ratio<sup>1, 11</sup>. CT findings in patients with MPC may show airspace ground-glass nodular opacities, dense consolidation, calcified nodules, reticular opacities, and chest wall vascular calcification. The most common reported HRCT finding in the lung of MPC is centrilobular ground-glass nodular opacities with numerous fluffy and poorly defined 3-10-mm nodules<sup>12,13</sup>, reflecting the deposition of calcium salts in the pulmonary interstitium. More severe interstitial calcification can result in dense areas of consolidation, which may be misdiagnosed as pulmonary edema or pneumonia<sup>14</sup>. Pulmonary microlithiasis, amiodarone toxicity, talcosis, iodinated oil embolism, and aspiration or extravasation of contrast material should be considered as differential diagnoses<sup>14,15</sup> for high-attenuated consolidation. In our case, patchy consolidation with a predominantly subpleural and peribroncheal

distribution may reflect OP <sup>16</sup>, additionally, a distinctive rim between the opacities and subpleural areas suggest NSIP/OP pattern, <sup>17</sup> which may reflect the fibroses and calcification alongside the bronchovascular bundles. High attenuation may reflect calcifications on the alveolar septa and reactive fibrotic changes in the pulmonary interstitium. The presence of high-attenuated areas of ectopic calcification of the myocardium at the side of the ventricular septum also suggests the diagnosis of MPC. Our patient demonstrated ALI in two weeks, due to OP; this represents an unusually rapid case (reported mean duration between onset and diagnosis of OP was 3.0 months)<sup>16</sup>. However, the fact that some patients progress to OP rapidly (shortest duration between onset and diagnosis of OP was 0.25 months) <sup>16</sup>, this rapid progression of alveolar fibroses in MPC with a myeloma patient<sup>14</sup> suggested that OP could develop in a short period in particular conditions. The chest abnormalities of MPC were reversible in our case, similar to a previously reported patient with multiple myeloma<sup>4</sup>.

<sup>99m</sup>Tc methylene diphosphonate bone scintigraphy is a more sensitive and

specific technique for MPC detection and is useful for early diagnosis<sup>18</sup>. The differential diagnoses of diffuse pulmonary uptake on bone scan other than MPC are malignant metastatic diseases (prostate, breast, lung, and renal cancer), haematological malignancies (Hodgkin's disease and non-Hodgkin's lymphoma), bone tumors and bone dysplasia, soft tissue sarcomas, paraneoplastic syndromes, rheumatologies, bone and joint infections, traumas, and metabolic bone diseases<sup>19</sup>. Diffuse pulmonary uptakes on bone scans may be caused by multiple lung calcifications; for a complete list of differential diagnoses, refer to Table 1. A patient's history, symptoms, clinical findings, CT and MRI findings, and further tissue analysis may help refine the diagnosis.

### Pathologic Discussion

Deposition of calcium salts in MPC predominantly occurs in the alveolar septa, with a particular affinity for elastic fibers. Deposits in small blood vessels, bronchi, and bronchioles<sup>14,20</sup> are also seen. These appear on

hematoxylin and eosin (HE) staining as basophilic granular or linear deposits, and Von Kossa staining is significantly more sensitive in detecting calcium in tissues<sup>1</sup>. In our case, multiple foci of OP were detected in the lungs, and extensive interstitial calcifications were observed along the alveolar septa, at the base of the areas of OP (Fig. 4B, 5A). Airspace organization may have occurred secondary to exudate release in response to interstitial injury and a desmoplastic reaction attributed to calcium deposition<sup>12</sup>. When calcium deposition is limited, it is only observed in the alveolar/capillary wall, and such injury may not occur. However, in fatal cases of progressing respiratory failure caused by MPC, excessive calcium deposition in the alveolar walls destroys the alveolar/capillary barrier, causing pulmonary edema and death<sup>21</sup>. Drug-induced pneumonia was not likely in our case because neither pneumocyte hyperplasia nor tissue eosinophilia was seen in the lungs. No evidence of pulmonary edema, congestive alveolar wall capillaries, or fluid in the alveolar space was noted. There were temporally different phases of fibroses, some of which were

chronic scars, suggesting the presence of subclinical injury related to preexisting calcifications before symptom appearance (Fig. 5B).

## Conclusion

A patient with myeloma presented with dyspnea and cough, along with progressive pulmonary opacities. He was diagnosed with MPC by transbronchial biopsy. Normalization of both calcium and phosphorus levels improved his symptoms, and the abnormal opacities disappeared in the lungs. The patient's lung histology captured desmoplastic changes in the alveolar septa, from multiple calcifications to interstitial fibrosis.

## Acknowledgment

Author contributions: Yamamoto K. cared for the patient and wrote the manuscript. Ando K. cared for and treated the patient. Tanaka M. prepared the table and figures for the manuscript. Yura H. and Sakamoto N. performed a bronchoscopy and biopsies for the patient. Zaizen Y. and

Fukuoka J. read pathological findings. Ashizawa K. read radiological findings. Miyazaki Y. and Mukae H. supervised and managed the patient's care.

## References

1. Chan ED, Morales DV, Welsh CH, McDermott MT, Schwarz MI. Calcium deposition with or without bone formation in the lung. *Am J Respir Crit Care Med.* 2002;165(12):1654-1669.
2. Crippa C, Ferrari S, Drera M, et al. Pulmonary calciphylaxis and metastatic calcification with acute respiratory failure in multiple myeloma. *J Clin Oncol.* 2010;28(9):e133-135.
3. Cagirgan S, Soyer N, Vural F, et al. Metastatic pulmonary calcinosis and leukocytoclastic vasculitis in a patient with multiple myeloma. *Turk J Haematol.* 2012;29(4):397-400.
4. Weber CK, Friedrich JM, Merkle E, et al. Reversible metastatic pulmonary calcification in a patient with multiple myeloma. *Ann Hematol.* 1996;72(5):329-332.
5. Oyajobi BO. Multiple myeloma/hypercalcemia. *Arthritis Res Ther.* 2007;9 Suppl 1:S4.
6. Teh SP, Ng YL, Yii CAA, Choong HLL, Wong J. Metastatic pulmonary calcification: Experience from a single center in Singapore. *Hemodial Int.* 2018;22(4):E63-E67.
7. Rapp RP, Kuhn R. Clinical pharmacetics and calcium ceftriaxone. *Ann Pharmacother.* 2007;41(12):2072.
8. Ishii H, Kai N, Kashima K, et al. Bronchoscopic and electron microscopic findings in a dialysis patient with metastatic pulmonary calcification. *Intern Med.* 2008;47(23):2099-2100.
9. Yasuo M, Tanabe T, Komatsu Y, et al. Progressive pulmonary calcification after successful renal transplantation. *Intern Med.* 2008;47(3):161-164.
10. Prince JS, Duhamel DR, Levin DL, Harrell JH, Friedman PJ. Nonneoplastic lesions of the tracheobronchial wall: radiologic findings with bronchoscopic correlation. *Radiographics.* 2002;22 Spec No:S215-230.
11. Belem LC, Zanetti G, Souza AS, Jr., et al. Metastatic pulmonary

- calcification: state-of-the-art review focused on imaging findings. *Respir Med.* 2014;108(5):668-676.
12. Hartman TE, Muller NL, Primack SL, et al. Metastatic pulmonary calcification in patients with hypercalcemia: findings on chest radiographs and CT scans. *AJR Am J Roentgenol.* 1994;162(4):799-802.
  13. Belem LC, Souza CA, Souza AS, Jr., et al. Metastatic pulmonary calcification: high-resolution computed tomography findings in 23 cases. *Radiol Bras.* 2017;50(4):231-236.
  14. Marchiori E, Muller NL, Souza AS, Jr., Escuissato DL, Gasparetto EL, de Cerqueira EM. Unusual manifestations of metastatic pulmonary calcification: high-resolution CT and pathological findings. *J Thorac Imaging.* 2005;20(2):66-70.
  15. Marchiori E, Franquet T, Gasparetto TD, Goncalves LP, Escuissato DL. Consolidation with diffuse or focal high attenuation: computed tomography findings. *J Thorac Imaging.* 2008;23(4):298-304.
  16. Zhou Y, Wang L, Huang M, et al. A long-term retrospective study of patients with biopsy-proven cryptogenic organizing pneumonia. *Chron Respir Dis.* 2019;16:1479973119853829.
  17. Travis WD, Costabel U, Hansell DM, et al. An official American Thoracic Society/European Respiratory Society statement: Update of the international multidisciplinary classification of the idiopathic interstitial pneumonias. *Am J Respir Crit Care Med.* 2013;188(6):733-748.
  18. Rajkovaca Z, Kovacevic P, Jakovljevic B, Eric Z. Detection of pulmonary calcification in haemodialysed patients by whole-body scintigraphy and the impact of the calcification to parameters of spirometry. *Bosn J Basic Med Sci.* 2010;10(4):303-306.
  19. Van den Wyngaert T, Strobel K, Kampen WU, et al. The EANM practice guidelines for bone scintigraphy. *Eur J Nucl Med Mol Imaging.* 2016;43(9):1723-1738.
  20. Ullmer E, Borer H, Sandoz P, Mayr M, Dalquen P, Soler M. Diffuse

- pulmonary nodular infiltrates in a renal transplant recipient. Metastatic pulmonary calcification. *Chest*. 2001;120(4):1394-1398.
21. Liou JH, Cho LC, Hsu YH. Paraneoplastic hypercalcemia with metastatic calcification--clinicopathologic studies. *Kaohsiung J Med Sci*. 2006;22(2):85-88.

Table 1. Causes of pulmonary calcification\*

<p>A. Neoplastic</p> <ol style="list-style-type: none"> <li>1. Parathyroid carcinoma</li> <li>2. Multiple myeloma</li> <li>3. Lymphoma/leukemia</li> <li>4. Hypopharyngeal carcinoma</li> <li>5. Synovial sarcoma</li> <li>6. Breast carcinoma</li> <li>7. Choriocarcinoma</li> <li>8. Osteogenic sarcoma</li> <li>9. Melanoma</li> </ol>	<p>C. Systemic disorders</p> <ol style="list-style-type: none"> <li>1. Amyloidosis</li> <li>2. Sarcoidosis</li> <li>3. Pulmonary alveolar microlithiasis</li> </ol>
<p>B. Endocrine &amp; Metabolic</p> <ol style="list-style-type: none"> <li>1. Chronic renal insufficiency on hemodialysis</li> <li>2. Hyperparathyroidism</li> </ol>	<p>D. Infections</p> <ol style="list-style-type: none"> <li>1. <i>Histoplasma capsulatum</i></li> <li>2. <i>Coccidioides immitis</i></li> <li>3. <i>Mycobacterium tuberculosis</i></li> <li>4. <i>Pneumocystis jirovecii</i></li> <li>5. <i>Paragonimus westermani</i></li> <li>6. Varicella-zoster virus</li> <li>7. Smallpox virus</li> </ol>

<p>3. Excess calcium and vitamin D (milk-alkali syndrome)</p> <p>4. Hypervitaminosis D</p> <p>5. Hemosiderosis</p> <p>6. Osteopetrosis</p> <p>7. Osteitis deformans (Paget's disease)</p>	<p>E. Vascular disorders</p> <p>1. Vascular grafts</p> <p>2. Pulmonary hypertension</p> <p>3. Congenital high flow</p> <p>F. Environmental</p> <p>1. Pneumoconiosis</p> <p>2. Asbestos</p> <p>G. Iatrogenic</p> <p>1. Orthotopic liver transplantation</p>
-----------------------------------------------------------------------------------------------------------------------------------------------------------------------------------------------	------------------------------------------------------------------------------------------------------------------------------------------------------------------------------------------------------------------------------------------------------------

\*Modified from reference (1)

## Figure legends

### Fig. 1

A: Anteroposterior chest radiograph obtained on respiratory failure onset showing dense areas of consolidation sparing right mid lung zone and bases, sternotomy clips, enlarged cardiac contour, subpleural opacities bilaterally, especially in the upper third of the lung zones, and small bilateral pleural effusions.

B: Anteroposterior chest radiograph obtained one week after parathyroid surgery. Sternotomy clips were seen, but there were no abnormal shadows in the lungs.

### Fig. 2

Non-contrast-enhanced chest CT images.

A: CT images with mediastinal window setting obtained on respiratory failure onset showing extensive consolidation with high attenuation in peripheral distribution in the bilateral lungs. Multiple pleural calcifications and calcifications of the myocardium at the side of the ventricular septum

were observed (arrow), as were bilateral pleural effusions.

B: HRCT images with lung window setting obtained on respiratory failure onset, showing diffuse dense consolidations with consolidation with air bronchograms in a peripheral distribution and small nodular ground-glass opacities.

C: HRCT image with lung window setting obtained 3 months after discharge showing that the consolidations and calcifications had disappeared in both lungs, but the ground-glass opacities remained.

Fig. 3

A, B: Bronchoscopic findings showing multiple small white deposits in the membranous portion of the trachea.

C.  $^{99m}\text{Tc}$  diphosphonate scintigraphy (anterior and posterior views). Diffuse accumulation in the thorax, with significant abnormal increased activity in the lungs and myocardium detected.

Fig. 4

A: The endobronchial mucosal biopsy specimen from the right upper bronchus B2a showed basophilic fine calcific substances along the thickened parabronchial interstitial space (HE staining, magnification  $\times 2, \times 10$ ).

B: The transbronchial lung biopsy specimen from the right lower lobe showed multiple organizing pneumonias that filled the air spaces, and multiple linear basophilic calcifications were detected along the peripheral lesion of those organizing pneumonia areas. Those calcifications were on the alveolar septa, which were thickened because of a desmoplastic reaction (HE staining, magnification  $\times 2, \times 10$ ).

Fig. 5

A: Extensive interstitial amorphous calcium salt deposits can be seen along the alveolar septa alongside the areas of organizing pneumonia (Von Kossa stain, magnification  $\times 2$ ).

B: Calcifications were detected at the stalks of polypoid organizations (Von Kossa, magnification  $\times 2$ ).

C: Acute or subacute fibrotic changes in the area of organizing pneumonia

(EVG, magnification ×2).

D: Chronic fibroses were seen next to the calcifications (HE, magnification ×10).

Fig.1

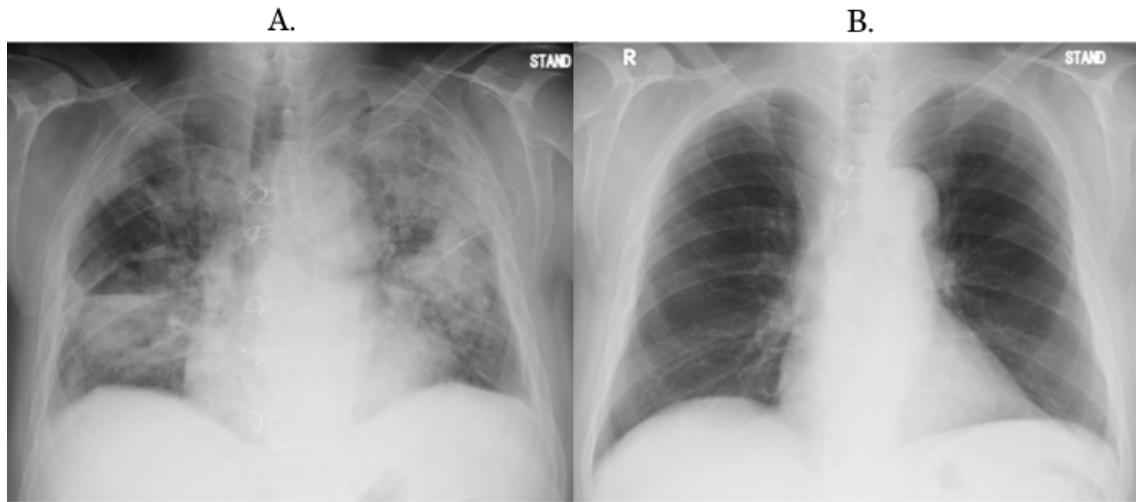


Fig.2

A.

B.

C.

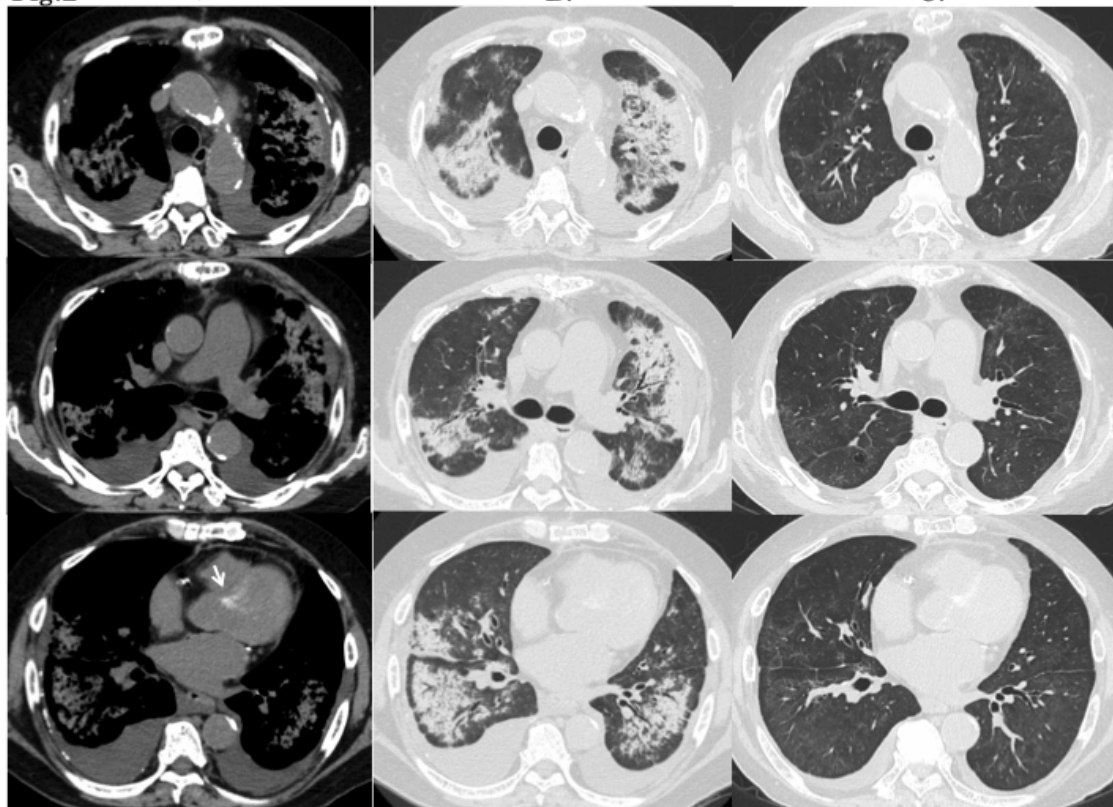


Fig.3

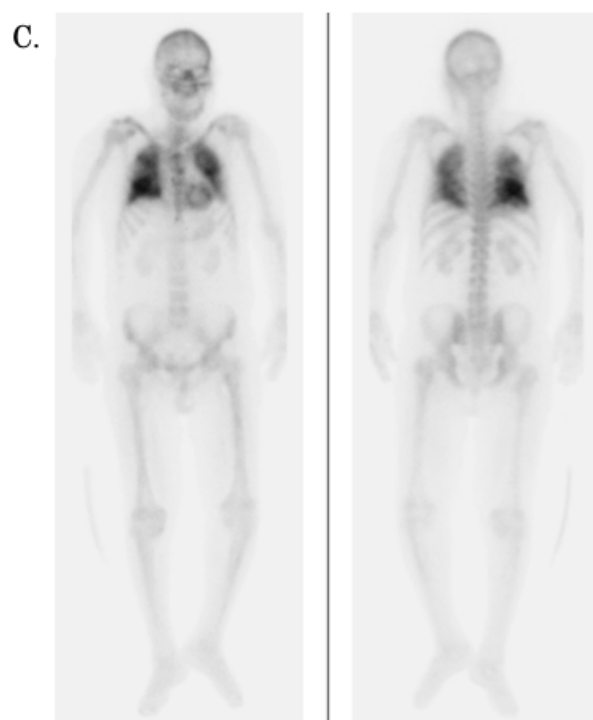
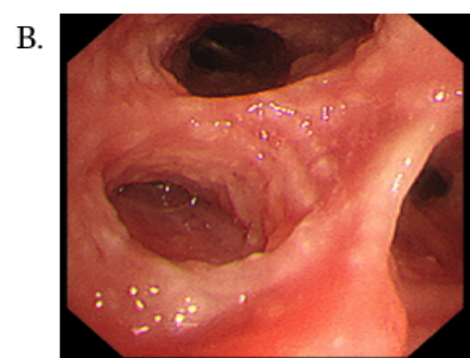
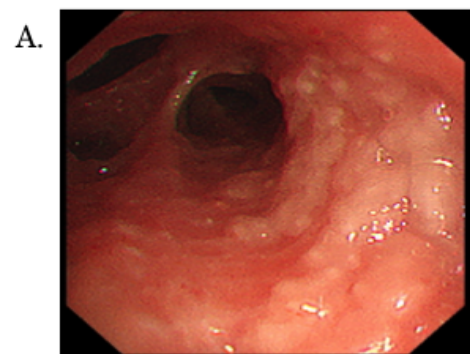
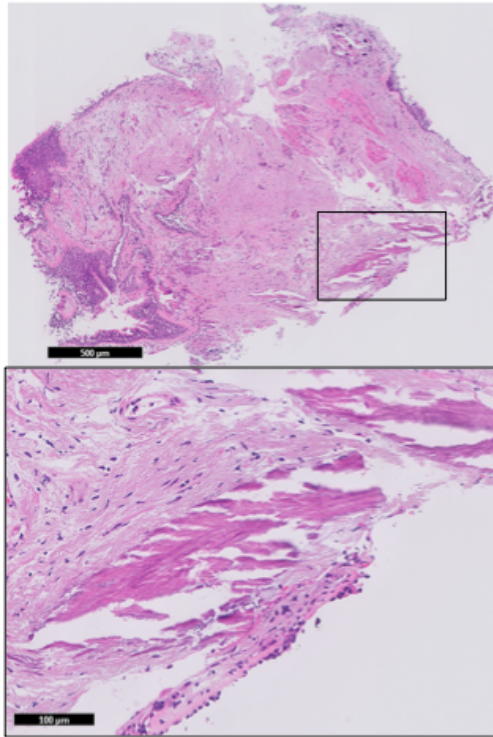


Fig.4

A.



B.

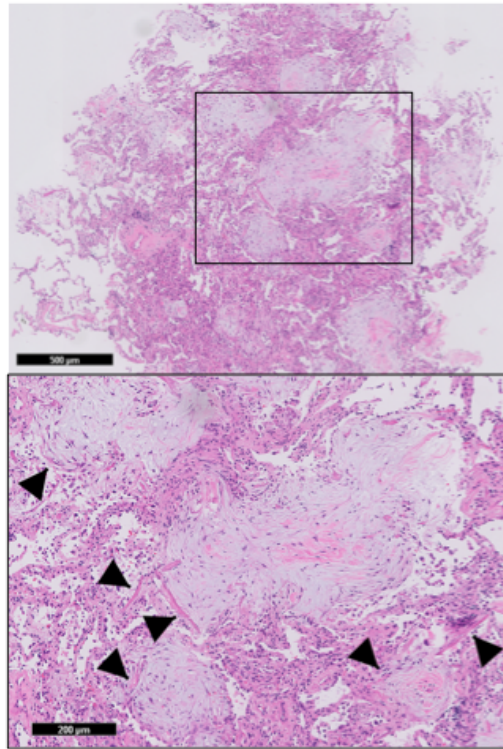
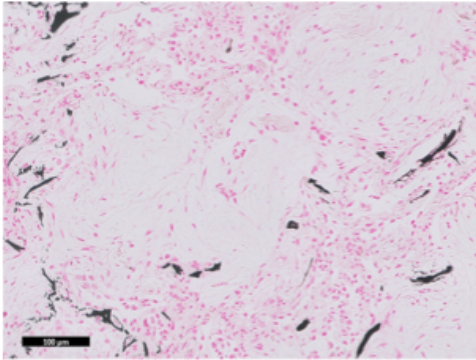
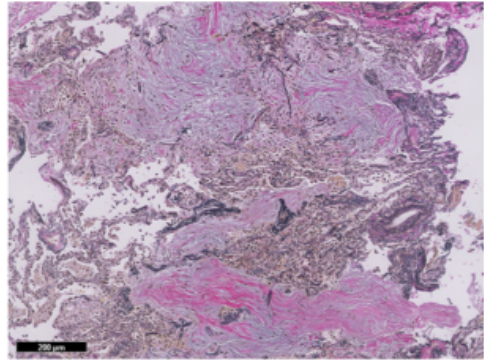


Fig.5

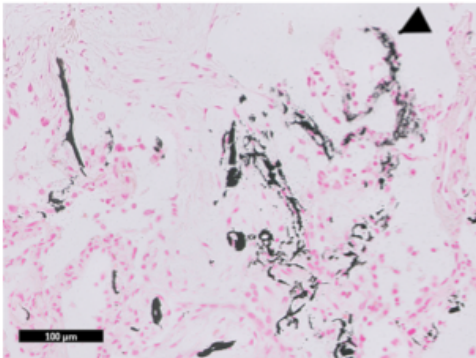
A.



C.



B.



D.

